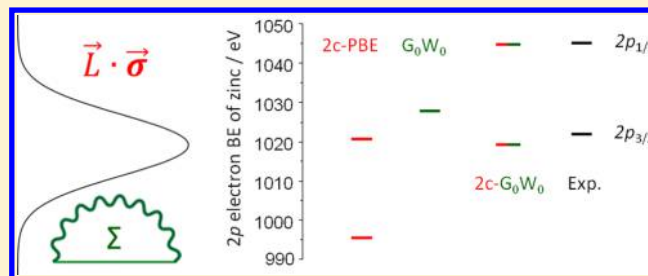


One-Electron Energies from the Two-Component GW Method

Michael Kühn[†] and Florian Weigend^{*,†,‡}[†]Institut für Physikalische Chemie, Karlsruher Institut für Technologie, Kaiserstraße 12, 76131 Karlsruhe, Germany[‡]Institut für Nanotechnologie, Karlsruher Institut für Technologie, Postfach 3640, 76021 Karlsruhe, Germany

S Supporting Information

ABSTRACT: The two-component extension of the G_0W_0 method for closed-shell systems based on the previously implemented one-component version in TURBOMOLE that uses localized basis functions is presented. In this way, it is possible to account for spin–orbit effects on one-electron energies of isolated molecular systems at the G_0W_0 level. We briefly sketch the derivation of the underlying equations, give details about the implementation, and apply the method to several atomic and diatomic systems. The influence of spin–orbit coupling changes calculated first ionization energies by up to 0.7 eV, leading to maximum errors smaller than 0.3 eV. Virtually the same results are obtained with an economic extrapolation scheme based on the one-component G_0W_0 and the two-component reference state calculation. Furthermore, for binding energies of core levels, two-component G_0W_0 is very accurate, as demonstrated for mercury and zinc atoms as well as for ZnF_2 .



1. INTRODUCTION

Experimentally measured quantities such as ionization energies (IEs), electron affinities (EAs), and core-level binding energies observable via X-ray photoelectron spectroscopy are commonly identified with quantum-chemically calculated one-electron energies (orbital energies). At the Hartree–Fock (HF) level, according to Koopmans' theorem, the first vertical IE is associated with the negative of the energy of the highest occupied molecular orbital (HOMO).¹ Despite this formal justification, the disadvantage remains that HF theory does not describe the effect of electron correlation. Kohn–Sham (KS) density functional theory (DFT), on one hand, approximately describes this effect via the exchange–correlation (XC) functional, but on the other hand, using these approximate (not self-interaction corrected) XC functionals, the negative of the HOMO energy is not close to the IE in many cases, although a DFT analog of Koopmans' theorem exists. Nevertheless, in practice, DFT orbital energies are often used for the description of vertical IEs, EAs, and binding energies in general.^{2–4} Sometimes, reasonable estimates for those quantities may be obtained using DFT orbital energies, but the approximations in the XC functionals (most notably in the exchange part, which is treated exactly within HF) often lead to unreliable results.^{5–7}

The GW approach^{5,8} improves upon the shortcomings of HF and DFT when considering one-electron energies: it subtracts the XC contribution and adds HF exchange along with a systematically derived part of the electron correlation contribution instead. The central quantity within the GW method is the one-electron Green's function, which is directly related to the process of photoemission and photoabsorption. Thus, the poles of this function by construction define one-electron energies (vertical IEs, EAs, and electron binding

energies in general). Overall, the GW approach has become a well-established method for the calculation of one-electron energies (i.e., the band structure) of solids and surfaces since it significantly improves the description of the electronic structure compared to that with HF and DFT.^{5,9,10}

Thus, the GW approach has become available in many plane-wave codes as a standard tool. Recent applications indicate that this method will also be successful when isolated systems are treated.^{11–27} The calculation of core-level binding energies, within GW and in general, is most efficiently done using atom-centered (Gaussian-type) basis functions. Despite the fact that such approaches are not novel,^{14–18,23,28–30} to the best of our knowledge, there are only two GW implementations into generic quantum chemistry program packages, namely, those into the FHI-aims code^{28,31} and into the TURBOMOLE program suite.^{32,33} The noniterative G_0W_0 implementation of van Setten et al. in the TURBOMOLE quantum chemistry package, which is based on localized basis sets using atom-centered Gaussian-type basis functions, yields results significantly better in agreement with the experiment (in the case of first vertical IE mostly within 0.6 eV, maximum absolute deviation of 1.2 eV) than those obtained from HF and DFT for a test set containing 27 molecules.³²

In particular, for heavy elements, one-electron energies (orbital energies) are significantly influenced by relativistic effects. Scalar relativistic effects described by the mass-velocity and Darwin term in the Hamiltonian, yield a shift, spin–orbit coupling (SOC) yields a splitting of one-electron energies. In past years, quantum-chemical methods have been extended to the relativistic framework. Usually, the incorporation of

Received: November 28, 2014

Published: February 5, 2015

relativistic effects is limited to scalar relativistic effects since, like in nonrelativistic theories, one-component scalar relativistic (1c) real molecular orbitals (MOs) can be used and thus the structure of an existing quantum-chemical program does not need to be changed. Most efficiently, these scalar relativistic effects are modeled by 1c effective core potentials (ECPs) covering the inner electrons, like is done, e.g., in the 1c G_0W_0 implementation of van Setten et al.³² One has to be aware that the effect of SOC, that leads to a splitting of the 1c orbital energies, is neglected. On the other hand, for a method that aims at the accurate calculation of one-electron energies, it is highly desirable to include this effect.

The most fundamental way to include SOC is by utilizing a fully relativistic formalism, e.g., based on the Dirac–Coulomb Hamiltonian, using four-component (4c) complex spinors. A more economic alternative, with a very similar accuracy, is a quasi-relativistic theory using two-component (2c) complex spinors. Within a 2c theory SOC (as well as 1c), contributions can be incorporated by the all-electron exact 2c (X2C) approach^{34–42} or more efficiently, but without explicitly describing the core levels, by 2c ECPs, e.g., 2c Dirac–Hartree–Fock ECPs (dhf-ECPs) that are fitted to 4c multiconfiguration Dirac–Hartree–Fock calculations on atoms and are available for elements beyond Kr.^{43–49}

Recently, several 2c methods based on ECPs and X2C have been implemented in the TURBOMOLE program suite that take into account the effect of SOC on molecular systems in a highly efficient manner: DFT and HF ground-state methods,⁵⁰ second-order Møller–Plesset perturbation theory (MP2),⁵¹ time-dependent density functional theory (TDDFT),⁵² and total ground-state correlation energies from the random phase approximation (RPA).⁵³

To the best of our knowledge, until now, the GW approach has been extended to the 4c and 2c framework including the effect of SOC only within the plane-wave formalism:^{54–58} Sakuma et al.⁵⁶ investigated the effect of SOC on the band structures of Hg chalcogenides and Kutepov et al.,⁵⁷ on the band structures of Pu and Am metals. Umari et al.⁵⁸ showed that the consideration of SOC effects on the band structures of $\text{CH}_3\text{NH}_3\text{PbI}_3$ and $\text{CH}_3\text{NH}_3\text{SnI}_3$ perovskites is important to assess their applicability in solar cells.

Therefore, the goal of this work is to extend the GW approach to a 2c formalism that can be used to calculate the effect of SOC on one-electron energies of molecular systems. To this end, we generalize the derivation of van Setten et al.³² and implement the resulting 2c G_0W_0 equations in the TURBOMOLE program suite for (Kramers-restricted) closed-shell systems exploiting our 2c TDDFT code.⁵²

The presented theory is fully operational for different 2c approaches (X2C, ECPs, ...) since all (one-electron) relativistic effects on one-electron energies within the G_0W_0 approximation arise from the corresponding reference-state spinors and their energies only. Thus, no extra relativistic contributions have to be taken into account in the equations. The derived formalism can also be easily extended to the 4c formalism based on the Dirac–Coulomb Hamiltonian.

The article is organized as follows. In Section 2, we briefly sketch the derivation of the equations needed to calculate the one-electron energies within the 2c G_0W_0 approach for (Kramers-restricted) closed-shell systems. Details of the implementation in the TURBOMOLE program suite are given in Section 3. In Section 4, the 2c G_0W_0 method is applied to the calculation of first IEs and EAs of several atomic

and diatomic systems as well as to the core-level splittings of Zn, ZnF_2 , and Hg. Results are compared to other 2c and 1c approaches as well as experimental data. In the Appendix, we show the connection between the 2c GW approach and total ground-state correlation energies obtained from 2c RPA.

2. THEORY

2.1. Two-Component Hedin Equations and G_0W_0 Approximation. Following the derivation presented by van Setten et al.,³² the starting point for the 2c GW method, which accounts for SOC effects on one-electron energies, is the equation of motion for the 2c one-electron Green's function \mathbf{G}^8

$$\begin{aligned} & \left[i\hbar \frac{\partial}{\partial t_1} \mathbf{1} - \hat{t}_1 \mathbf{1} - \hat{v}_H(\vec{r}_1) \mathbf{1} - \hat{v}(\vec{r}_1) \right] \mathbf{G}(\vec{r}_1, t_1, \vec{r}_2, t_2) \\ & - \int d^3r_3 dt_3 \Sigma(\vec{r}_1, t_1, \vec{r}_3, t_3) \mathbf{G}(\vec{r}_3, t_3, \vec{r}_2, t_2) \\ & = \delta^3(\vec{r}_1 - \vec{r}_2) \delta(t_1 - t_2) \mathbf{1} \end{aligned} \quad (1)$$

\hat{t}_1 is the 1c kinetic energy operator for electron 1 and \hat{v}_H is the bare 1c Hartree (or Coulomb) potential. $\mathbf{1}$ is the 2×2 identity matrix in spin space, and δ denotes the Dirac delta distribution. \hat{v} is the common 1c one-electron external potential (Coulomb interaction between electron and all nuclei) that additionally contains effective one-electron relativistic potentials, in particular the 2c SOC contribution, which is nondiagonal in spin space. In the 1c limit, the diagonal $\hat{v} \mathbf{1}$ appears instead of \hat{v} since the SOC contribution is not taken into account. The 2c one-electron Green's function $\mathbf{G}(\vec{r}_1, t_1, \vec{r}_2, t_2)$ describes the probability for an electron that was created at (\vec{r}_2, t_2) to be picked up at (\vec{r}_1, t_1) (influence of SOC included) and is therefore directly related to the processes of photoemission and photoabsorption. One-electron energies (and lifetimes) are obtained from the poles of \mathbf{G} .

The interacting (\mathbf{G}) and noninteracting (\mathbf{G}_H) 2c one-electron Green's function, the latter of which is calculated with respect to the Hartree ground state, are connected via the Dyson equation

$$\begin{aligned} \mathbf{G}(\vec{r}_1, t_1, \vec{r}_2, t_2) &= \mathbf{G}_H(\vec{r}_1, t_1, \vec{r}_2, t_2) + \int d^3r_3 dt_3 d^3r_4 dt_4 \\ &\times \mathbf{G}_H(\vec{r}_1, t_1, \vec{r}_3, t_3) \Sigma(\vec{r}_3, t_3, \vec{r}_4, t_4) \mathbf{G}(\vec{r}_4, t_4, \vec{r}_2, t_2) \end{aligned} \quad (2)$$

Equation 2 along with

$$\begin{aligned} \Sigma(\vec{r}_1, t_1, \vec{r}_2, t_2) &= i \int d^3r_3 dt_3 d^3r_4 dt_4 \mathbf{G}(\vec{r}_1, t_1, \vec{r}_3, t_3 + \eta) \\ &\times \Gamma(\vec{r}_3, t_3, \vec{r}_2, t_2, \vec{r}_4, t_4) W(\vec{r}_1, t_1, \vec{r}_4, t_4) \mathbf{1} \end{aligned} \quad (3)$$

$$\begin{aligned} W(\vec{r}_1, t_1, \vec{r}_2, t_2) &= \hat{v}_{ee}(\vec{r}_1 - \vec{r}_2) \delta(t_1 - t_2) + \int d^3r_3 dt_3 d^3r_4 \\ &\times dt_4 \hat{v}_{ee}(\vec{r}_1 - \vec{r}_3) \delta(t_1 - t_3) P(\vec{r}_3, t_3, \vec{r}_4, t_4) \\ &\times W(\vec{r}_4, t_4, \vec{r}_2, t_2) \end{aligned} \quad (4)$$

$$\begin{aligned} P(\vec{r}_1, t_1, \vec{r}_2, t_2) &= -i \int d^3r_3 dt_3 d^3r_4 dt_4 \mathbf{G}(\vec{r}_1, t_1, \vec{r}_3, t_3) \\ &\times \Gamma(\vec{r}_3, t_3, \vec{r}_2, t_2, \vec{r}_4, t_4) \mathbf{G}(\vec{r}_4, t_4, \vec{r}_1, t_1 + \eta) \end{aligned} \quad (5)$$

and

$$\begin{aligned} \Gamma(\vec{r}_1, t_1, \vec{r}_2, t_2, \vec{r}_3, t_3) &= \delta^3(\vec{r}_1 - \vec{r}_2) \delta(t_1 - t_2) \delta^3(\vec{r}_2 - \vec{r}_3) \\ &\times \delta(t_2 - t_3) \mathbf{1} + \int d^3r_4 dt_4 d^3r_5 dt_5 d^3r_6 dt_6 d^3r_7 dt_7 \\ &\times \frac{\delta \Sigma(\vec{r}_1, t_1, \vec{r}_2, t_2)}{\delta \mathbf{G}(\vec{r}_4, t_4, \vec{r}_5, t_5)} \mathbf{G}(\vec{r}_4, t_4, \vec{r}_6, t_6) \\ &\times \Gamma(\vec{r}_6, t_6, \vec{r}_7, t_7, \vec{r}_3, t_3) \mathbf{G}(\vec{r}_7, t_7, \vec{r}_5, t_5) \end{aligned} \quad (6)$$

are the 2c Hedin equations^{5,8} that dictate the procedure for obtaining the exact 2c interacting one-electron Green's function \mathbf{G} under the assumption of a spin-independent (i.e., non-relativistic) Coulomb interaction between the electrons, $\hat{v}_{ee}(\vec{r}_1 - \vec{r}_2) = 1/|\vec{r}_1 - \vec{r}_2|$, in eq 4.⁵⁷ Equation 3 defines the 2c self-energy Σ in terms of the dynamically screened Coulomb interaction W , which is diagonal in spin-space due to the spin-independent structure of the interelectronic interaction, and the 2c vertex operator Γ . η denotes a positive real infinitesimal. Equation 4 relates W to the Coulomb interaction \hat{v}_{ee} and the polarization function P . The latter is obtained via eq 5. Equation 6 is the 2c Bethe–Salpeter equation.

Upon neglecting the last term in the Bethe–Salpeter equation (eq 6), the GW approximation is obtained as in the 1c case. As a result, eq 3 reads in energy space

$$\begin{aligned} \Sigma[\mathbf{G}](\vec{r}_1, \vec{r}_2, E) &= \frac{i}{2\pi} \int_{-\infty}^{\infty} d\nu e^{-i\nu\eta} \mathbf{G}(\vec{r}_1, \vec{r}_2, E - \nu) \\ &\times W(\vec{r}_1, \vec{r}_2, \nu) \mathbf{1} \end{aligned} \quad (7)$$

The 2c self-energy Σ describes exchange and correlation effects under the influence of SOC. It is a functional of \mathbf{G} , which is similar to 2c DFT,^{50,59} where the (noncollinear) XC potential \hat{v}_{XC} is a functional of the ground-state total electron density ρ (and the noncollinear spin density s); therefore, the respective equations have to be solved iteratively. However, similar to the HF exchange and unlike (semi) local XC potentials in DFT, Σ is nonlocal in space. Furthermore, Σ depends on the energy E .

Instead of a fully self-consistent 2c GW solution, we consider the so-called G_0W_0 approximation,³² where eq 7 is evaluated only once. In this case, the question arises as to which reference should be chosen to calculate \mathbf{G} and W , since only a fully self-consistent solution will be independent of the choice of reference. It has been argued that a KS reference yields final results within the G_0W_0 approximation, which are usually close to the fully self-consistent GW solution.^{32,60,61} Using a 2c KS reference, the 2c one-electron Green's function is given as

$$\begin{aligned} \mathbf{G}_{\text{KS}}(\vec{r}_1, \vec{r}_2, E) &= \sum_{\vec{\sigma}} \sum_{i=1}^{N_{\vec{\sigma}}} \frac{\Phi_{i\vec{\sigma}}(\vec{r}_1) \Phi_{i\vec{\sigma}}^{\dagger}(\vec{r}_2)}{E - \epsilon_{i\vec{\sigma}} - i\eta} \\ &+ \sum_{\vec{\tau}} \sum_{a=N_{\vec{\sigma}}+1}^{M_{\vec{\tau}}} \frac{\Phi_{a\vec{\tau}}(\vec{r}_1) \Phi_{a\vec{\tau}}^{\dagger}(\vec{r}_2)}{E - \epsilon_{a\vec{\tau}} + i\eta} \end{aligned} \quad (8)$$

where $\Phi_{p\vec{\sigma}}$ is a 2c complex spinor with energy $\epsilon_{p\vec{\sigma}}$. Indices i, j, \dots are used for occupied, a, b, \dots for virtual and p, q, \dots for general molecular spinors. Greek indices $\vec{\sigma}, \vec{\tau}, \vec{\sigma}', \vec{\tau}', \vec{\nu} \in \{\vec{\alpha}, \vec{\beta}\}$ refer to 2c time-reversal symmetry-adapted Kramers partners describing $N_{\vec{\alpha}}$ moment-up ($\vec{\alpha}$) and $N_{\vec{\beta}}$ moment-down ($\vec{\beta}$) electrons. The total number of spinors (occupied plus virtual) is $M_{\vec{\alpha}} = N_{\vec{\alpha}} + N_{\vec{\alpha}}^{\text{virt}}$ and $M_{\vec{\beta}} = N_{\vec{\beta}} + N_{\vec{\beta}}^{\text{virt}}$, respectively. In the 1c limit, moment-up/moment-down ($\vec{\alpha}/\vec{\beta}$) electrons become ordinary spin-up/spin-down (α/β) electrons. As a result, the MOs $\Phi_{p\vec{\nu}}$ can be chosen to be real and eigenfunctions of \hat{S}_z .

It is convenient to express the dynamically screened Coulomb interaction W (eq 4) in terms of the density–density response function χ

$$\begin{aligned} W(\vec{r}_1, \vec{r}_2, \nu) &= \hat{v}_{ee}(\vec{r}_1 - \vec{r}_2) + \int d^3r_3 d^3r_4 \hat{v}_{ee}(\vec{r}_1 - \vec{r}_3) \\ &\times \chi(\vec{r}_3, \vec{r}_4, \nu) \hat{v}_{ee}(\vec{r}_4 - \vec{r}_2) \end{aligned} \quad (9)$$

χ can be obtained from 2c response theory in particular within the 2c RPA, which is meant to be identical to 2c time-dependent Hartree (TDH) theory in this case (Section 2.2), based on a 2c KS reference.⁵³

2.2. Two-Component Time-Dependent Hartree Theory. The density–density response function χ can be calculated from the general 2c non-Hermitian time-dependent Kohn–Sham (TDKS) eigenvalue problem for excitation energies ω_n ($n = 1, 2, 3, \dots$)^{52,62–64}

$$\begin{aligned} &\begin{pmatrix} A_{i\vec{\sigma}a\vec{\tau}j\vec{\sigma}'b\vec{\tau}'} & B_{i\vec{\sigma}a\vec{\tau}j\vec{\sigma}'b\vec{\tau}'} \\ (B_{i\vec{\sigma}a\vec{\tau}j\vec{\sigma}'b\vec{\tau}'})^* & (A_{i\vec{\sigma}a\vec{\tau}j\vec{\sigma}'b\vec{\tau}'})^* \end{pmatrix} \begin{pmatrix} X_{j\vec{\sigma}'b\vec{\tau}',n} \\ Y_{j\vec{\sigma}'b\vec{\tau}',n} \end{pmatrix} \\ &= \omega_n \begin{pmatrix} 1 & 0 \\ 0 & -1 \end{pmatrix} \begin{pmatrix} X_{i\vec{\sigma}a\vec{\tau},n} \\ Y_{i\vec{\sigma}a\vec{\tau},n} \end{pmatrix} \end{aligned} \quad (10)$$

where the Einstein summation convention is utilized. The (de)excitation vectors $X_{i\vec{\sigma}a\vec{\tau},n}$ and $Y_{i\vec{\sigma}a\vec{\tau},n}$ satisfy the normalization constraint

$$\begin{pmatrix} X_{i\vec{\sigma}a\vec{\tau},n} \\ Y_{i\vec{\sigma}a\vec{\tau},n} \end{pmatrix}^{\dagger} \begin{pmatrix} 1 & 0 \\ 0 & -1 \end{pmatrix} \begin{pmatrix} X_{i\vec{\sigma}a\vec{\tau},n} \\ Y_{i\vec{\sigma}a\vec{\tau},n} \end{pmatrix} = 1 \quad (11)$$

Within 2c RPA (2c TDH theory), the complex (Hermitian) orbital rotation Hessians are defined as

$$A_{i\vec{\sigma}a\vec{\tau}j\vec{\sigma}'b\vec{\tau}'}^{\text{RPA}} = (\epsilon_{a\vec{\tau}} - \epsilon_{i\vec{\sigma}}) \delta_{ij} \delta_{ab} \delta_{\vec{\sigma}\vec{\sigma}'} \delta_{\vec{\tau}\vec{\tau}'} + C_{i\vec{\sigma}a\vec{\tau}j\vec{\sigma}'b\vec{\tau}'}^{\text{RPA}} \quad (12)$$

$$B_{i\vec{\sigma}a\vec{\tau}j\vec{\sigma}'b\vec{\tau}'}^{\text{RPA}} = C_{i\vec{\sigma}a\vec{\tau}b\vec{\tau}'j\vec{\sigma}'}^{\text{RPA}} \quad (13)$$

with the coupling matrix

$$C_{i\vec{\sigma}a\vec{\tau}j\vec{\sigma}'b\vec{\tau}'}^{\text{RPA}} = \langle \Phi_{i\vec{\sigma}} \Phi_{b\vec{\tau}'} | \Phi_{a\vec{\tau}} \Phi_{j\vec{\sigma}'} \rangle \quad (14)$$

δ_{pq} is the Kronecker delta. Within 2c RPA (2c TDH theory), the coupling matrix (eq 14) contains just the (two-electron) Coulomb matrix elements in Dirac notation. Since only *one-electron* relativistic potentials are included in the Hamiltonian (\hat{v} in eq 1) accounting for SOC, they do not respond to a TD external perturbation. As a result, there is no additional SOC contribution to the coupling matrix, and SOC effects on excitations arise via the reference-state spinors and their energies only.

Starting from here, with an eye toward a computationally efficient implementation, only (Kramers-restricted) closed-shell systems are considered, for which eq 10 can be transformed to a Hermitian eigenvalue problem⁵³

$$\Omega_{i\vec{\sigma}a\vec{\tau}j\vec{\sigma}'b\vec{\tau}'}^{\text{RPA}} (X + Y)_{j\vec{\sigma}'b\vec{\tau}',n}^{\text{RPA}} = (\omega_n^{\text{RPA}})^2 (X + Y)_{i\vec{\sigma}a\vec{\tau},n}^{\text{RPA}} \quad (15)$$

with

$$\begin{aligned} \Omega_{i\vec{\sigma}a\vec{\tau}j\vec{\sigma}'b\vec{\tau}'}^{\text{RPA}} &= (\epsilon_{a\vec{\tau}} - \epsilon_{i\vec{\sigma}})^2 \delta_{ij} \delta_{ab} \delta_{\vec{\sigma}\vec{\sigma}'} \delta_{\vec{\tau}\vec{\tau}'} + 2\sqrt{\epsilon_{a\vec{\tau}} - \epsilon_{i\vec{\sigma}}} \\ &\times C_{i\vec{\sigma}a\vec{\tau}j\vec{\sigma}'b\vec{\tau}'}^{\text{RPA}} \sqrt{\epsilon_{b\vec{\tau}'} - \epsilon_{j\vec{\sigma}'}} \end{aligned} \quad (16)$$

The transformation to eq 15 is exact in case of 2c RPA (coupling matrix from eq 14).⁵³ We note that in the case of 2c TDDFT, where the noncollinear XC contribution is added to the coupling matrix, eq 15 is only approximate.^{52,63,64}

The transition density is then calculated using the converged $(X + Y)_{i\bar{\sigma}a\bar{\tau},n}^{\text{RPA}}$ and ω_n^{RPA} as

$$\rho_{0n}^{\text{RPA}}(\vec{r}) = \sum_{\bar{\sigma}\bar{\tau}} \sum_{i=1}^{N/2} \sum_{a=N/2+1}^{M/2} \frac{1}{\sqrt{\omega_n^{\text{RPA}}}} \sqrt{\epsilon_{a\bar{\tau}} - \epsilon_{i\bar{\sigma}}} \times (X + Y)_{i\bar{\sigma}a\bar{\tau},n}^{\text{RPA}} \Phi_{a\bar{\tau}}^{\dagger}(\vec{r}) \Phi_{i\bar{\sigma}}(\vec{r}) \quad (17)$$

For a (Kramers-restricted) closed-shell system $N_{\bar{\alpha}} = N_{\bar{\beta}} = (N/2)$ and $\epsilon_{p\bar{\alpha}} = \epsilon_{p\bar{\beta}}$ since the Kramers partners $\Phi_{p\bar{\alpha}}$ and $\Phi_{p\bar{\beta}}$ are either both occupied or unoccupied. Finally, the density–density response function can be expressed entirely in terms of *all* one-electron transition densities along with *all* excitation energies (within a given basis set) available from 2c RPA (2c TDH theory) via the Lehmann representation⁶⁵

$$\chi^{\text{RPA}}(\vec{r}_1, \vec{r}_2, \nu) = - \sum_n \left[\frac{\rho_{0n}^{\text{RPA}}(\vec{r}_1) (\rho_{0n}^{\text{RPA}}(\vec{r}_2))^*}{\omega_n^{\text{RPA}} - \nu - i\eta} + \frac{\rho_{0n}^{\text{RPA}}(\vec{r}_1) (\rho_{0n}^{\text{RPA}}(\vec{r}_2))^*}{\omega_n^{\text{RPA}} + \nu + i\eta} \right] \quad (18)$$

2.3. One-Electron Energies from the Two-Component Quasi-Particle Equations. One-electron energies under the influence of SOC within the G_0W_0 approximation are obtained via the 2c quasi-particle equations. They are similar to the 2c KS equations but with the XC potential (for Kramers-restricted closed-shell systems: $\hat{v}_{\text{XC}}[\rho]$) replaced by the self-energy. For the 2c G_0W_0 , one proceeds in the same way as described in the work of van Setten et al. for the 1c case:³² first, the 2c spinors appearing in the 2c quasi-particle equations are approximated by the 2c KS reference spinors. Second, the resulting equation is linearized. Third, the real part of the equation is considered, finally yielding the corrected one-electron energies within the 2c G_0W_0 approximation as^{5,32}

$$\epsilon_{p\bar{\nu}}^{G_0W_0} = \epsilon_{p\bar{\nu}} + \mathcal{R}(Z_{p\bar{\nu}}) \left[\underbrace{(1 - c_X) \langle \Phi_{p\bar{\nu}} | \Sigma_X | \Phi_{p\bar{\nu}} \rangle}_{\Delta\epsilon_{p\bar{\nu}}} + \mathcal{R} \left(\langle \Phi_{p\bar{\nu}} | \Sigma_C^{\text{RPA}}(\epsilon_{p\bar{\nu}}) | \Phi_{p\bar{\nu}} \rangle \right) - \langle \Phi_{p\bar{\nu}} | \hat{v}_{\text{XC}} \mathbf{1} | \Phi_{p\bar{\nu}} \rangle \right], \quad (19)$$

where the 2c self-energy from eq 7 was divided into an exchange part (Σ_X) stemming from the first term and an $\epsilon_{p\bar{\nu}}$ -dependent correlation part (Σ_C) stemming from the last term in eq 9. \mathcal{R} denotes the real part, and c_X is a hybrid mixing parameter (for $c_X = 0$ a pure 2c KS reference was used, for $c_X = 1$ a 2c HF reference).

Evaluation of the exchange part using eq 7 with a spectral representation of eq 8⁶⁵ and the first term in eq 9 yields³²

$$\langle \Phi_{p\bar{\nu}} | \Sigma_X | \Phi_{p\bar{\nu}} \rangle = - \sum_{\bar{\sigma}} \sum_{i=1}^{N/2} \langle \Phi_{p\bar{\sigma}} \Phi_{i\bar{\sigma}} | \Phi_{i\bar{\sigma}} \Phi_{p\bar{\nu}} \rangle \quad (20)$$

which is identical to the HF exchange.

Similarly, the correlation part is evaluated using eq 7 with a spectral representation of eq 8⁶⁵ and the second term in eq 9 with the density–density response function from 2c RPA (2c TDH theory) from eq 18 as³²

$$\mathcal{R}(\langle \Phi_{p\bar{\nu}} | \Sigma_C^{\text{RPA}}(\epsilon_{p\bar{\nu}}) | \Phi_{p\bar{\nu}} \rangle) = \sum_n \left[\sum_{\bar{\sigma}} \sum_{i=1}^{N/2} |\langle \Phi_{i\bar{\sigma}} \Phi_{p\bar{\nu}} | \rho_{0n}^{\text{RPA}} \rangle|^2 \frac{\epsilon_{p\bar{\nu}} - \epsilon_{i\bar{\sigma}} + \omega_n^{\text{RPA}}}{(\epsilon_{p\bar{\nu}} - \epsilon_{i\bar{\sigma}} + \omega_n^{\text{RPA}})^2 + \eta^2} + \sum_{\bar{\tau}} \sum_{a=N/2+1}^{M/2} |\langle \Phi_{a\bar{\tau}} \Phi_{p\bar{\nu}} | \rho_{0n}^{\text{RPA}} \rangle|^2 \frac{\epsilon_{p\bar{\nu}} - \epsilon_{a\bar{\tau}} - \omega_n^{\text{RPA}}}{(\epsilon_{p\bar{\nu}} - \epsilon_{a\bar{\tau}} - \omega_n^{\text{RPA}})^2 + \eta^2} \right] \quad (21)$$

The matrix elements are given in Mulliken notation and $\eta = 2\eta$. It should be emphasized at this point that *all* excitations n (within a given basis set) need to be calculated according to Section 2.2 for the evaluation of the correlation part of the 2c self-energy. $(\Phi_{i\bar{\sigma}} \Phi_{p\bar{\nu}} | \rho_{0n}^{\text{RPA}})$ is calculated using eq 17 (in Dirac notation) as

$$(\Phi_{i\bar{\sigma}} \Phi_{p\bar{\nu}} | \rho_{0n}^{\text{RPA}}) = \sum_{\bar{\sigma}'\bar{\tau}'} \sum_{j=1}^{N/2} \sum_{b=N/2+1}^{M/2} \langle \Phi_{i\bar{\sigma}} \Phi_{b\bar{\tau}'} | \Phi_{p\bar{\nu}} \Phi_{j\bar{\sigma}'} \rangle \times \sqrt{\frac{\epsilon_{b\bar{\tau}'} - \epsilon_{j\bar{\sigma}'}}{\omega_n^{\text{RPA}}}} (X + Y)_{j\bar{\sigma}'b\bar{\tau}',n}^{\text{RPA}} \quad (22)$$

In eq 19, $\mathcal{R}(Z_{p\bar{\nu}})$ appears due to the linearization and is given as

$$\mathcal{R}(Z_{p\bar{\nu}}) = \left[1 - \mathcal{R} \left(\left\langle \Phi_{p\bar{\nu}} \left| \frac{d\Sigma_C^{\text{RPA}}(E)}{dE} \right| \Phi_{p\bar{\nu}} \right\rangle \right) \right]^{-1} \quad (23)$$

with the real part of the diagonal matrix elements of the energy derivative of the correlation part of the 2c self-energy

$$\mathcal{R} \left(\left\langle \Phi_{p\bar{\nu}} \left| \frac{d\Sigma_C^{\text{RPA}}(E)}{dE} \right| \Phi_{p\bar{\nu}} \right\rangle \right) = \sum_n \left[\sum_{\bar{\sigma}} \sum_{i=1}^{N/2} |\langle \Phi_{i\bar{\sigma}} \Phi_{p\bar{\nu}} | \rho_{0n}^{\text{RPA}} \rangle|^2 \frac{\tilde{\eta}^2 - (\epsilon_{p\bar{\nu}} - \epsilon_{i\bar{\sigma}} + \omega_n^{\text{RPA}})^2}{[(\epsilon_{p\bar{\nu}} - \epsilon_{i\bar{\sigma}} + \omega_n^{\text{RPA}})^2 + \tilde{\eta}^2]^2} + \sum_{\bar{\tau}} \sum_{a=N/2+1}^{M/2} |\langle \Phi_{a\bar{\tau}} \Phi_{p\bar{\nu}} | \rho_{0n}^{\text{RPA}} \rangle|^2 \frac{\tilde{\eta}^2 - (\epsilon_{p\bar{\nu}} - \epsilon_{a\bar{\tau}} - \omega_n^{\text{RPA}})^2}{[(\epsilon_{p\bar{\nu}} - \epsilon_{a\bar{\tau}} - \omega_n^{\text{RPA}})^2 + \tilde{\eta}^2]^2} \right] \quad (24)$$

The final result, eq 19, strongly resembles the equation obtained within the 1c framework.³² In contrast to the 1c method, the one-electron functions $\Phi_{p\bar{\nu}}$ are 2c complex spinors instead of 1c real MOs. Thus, they are obtained along with the corresponding energies $\epsilon_{p\bar{\nu}}$ from a 2c instead of 1c KS reference-state calculation. In eq 19, no additional SOC contribution appears. Thus, SOC effects on one-electron energies $\epsilon_{p\bar{\nu}}^{G_0W_0}$ arise via $\Phi_{p\bar{\nu}}$ and $\epsilon_{p\bar{\nu}}$ only. These equations can also be easily extended to the fully relativistic 4c formalism based on the Dirac–Coulomb Hamiltonian simply by replacing all 2c quantities with their 4c analogs.⁵⁷ In the event that spin-dependent interactions between the electrons (\hat{v}_{ee}) are considered (i.e., as present within a theory based on the Dirac–Coulomb–Breit Hamiltonian), generalized Hedin equations have to be chosen in Section 2.1 as the starting point.^{54,55}

As an alternative to the linearized procedure, $\epsilon_{p\bar{\nu}}^{G_0W_0}$ can be calculated self-consistently. For this purpose, $\Delta\epsilon_{p\bar{\nu}}$ in eq 19 obtained for a given set of $\epsilon_{p\bar{\nu}}$ is added to $\epsilon_{p\bar{\nu}}$ and the result is used to recalculate $\Delta\epsilon_{p\bar{\nu}}$. This is repeated until convergence is

reached. If the integrals, see eq 22, are kept in memory (or stored on disk), then the additional effort for this iterative procedure is almost negligible.

3. IMPLEMENTATION

The calculation of the one-electron energies $\varepsilon_{p\bar{0}}^{G_0W_0}$ for (Kramers-restricted) closed-shell systems within the G_0W_0 approximation under the influence of SOC is performed in three steps:³² first, a 2c (KS) ground-state calculation⁵⁰ is performed, yielding the 2c spinors $\Phi_{p\bar{0}}$ and their energies $\varepsilon_{p\bar{0}}$. Second, a 2c RPA (2c TDH) calculation is performed as described in Section 2.2 using our recently implemented 2c TDDFT algorithm.⁵² As a result, *all* excitation energies ω_n^{RPA} along with *all* corresponding $(X + Y)_{j\bar{\sigma}'a\bar{\tau}',n}^{\text{RPA}}$ (within a given basis set) are obtained. Finally, the one-electron energies $\varepsilon_{p\bar{0}}^{G_0W_0}$ are calculated according to Section 2.3.

To this end, eqs 19–24 were implemented in the ESCF excited-state module^{32,52,66,67} of the TURBOMOLE program suite,³³ mainly by extending the already existing 1c routines³² to the 2c formalism. Both the HF exchange (eq 20) and the XC contribution in eq 19 need to be calculated in a 2c HF and 2c DFT calculation, respectively.⁵⁰ Thus, the calculation of those contributions within a 2c G_0W_0 procedure is done simply by calling existing routines. For the calculation of the correlation part of the 2c self-energy (eq 22), routines available from our recently implemented 2c TDDFT code⁵² need to be slightly modified. Finally, the sums in eqs 21 and 24 are evaluated by calling existing 1c G_0W_0 routines.

In the following, we describe how the central quantity, $(\Phi_{i\bar{\sigma}}\Phi_{p\bar{0}}|\rho_{0n}^{\text{RPA}})$ (eq 22), is calculated in our code, which is based on real atom-centered Gaussian-type basis functions ξ_μ ($\mu = 1, 2, \dots, N_{\text{BF}}$) that are used to expand the 2c spinors

$$\Phi_{p\bar{0}}(\vec{r}) = \sum_{\mu=1}^{N_{\text{BF}}} \begin{pmatrix} c_{\mu p\bar{0}}^\alpha \\ c_{\mu p\bar{0}}^\beta \end{pmatrix} \xi_\mu(\vec{r}) \quad (25)$$

$c_{\mu p\bar{0}}^\alpha$ and $c_{\mu p\bar{0}}^\beta$ are complex expansion coefficients. From now on, we suppress the RPA superscripts as well as the limits of the summations. Equation 22 is evaluated in four steps. First, the complex $(X + Y)_{j\bar{\sigma}'b\bar{\tau}',n}$ are multiplied by the real $\sqrt{\frac{\varepsilon_{b\bar{\tau}'} - \varepsilon_{j\bar{\sigma}'}}{\omega_n}}$ (both are the result of the preceding 2c RPA (2c TDH) calculation)

$$(X + Y)_{j\bar{\sigma}'b\bar{\tau}',n} = \sqrt{\frac{\varepsilon_{b\bar{\tau}'} - \varepsilon_{j\bar{\sigma}'}}{\omega_n}} (X + Y)_{j\bar{\sigma}'b\bar{\tau}',n} \quad (26)$$

Second, $(X + Y)_{j\bar{\sigma}'b\bar{\tau}',n}$ is transformed to the basis given by ξ_μ ($\mu = 1, 2, \dots, N_{\text{BF}}$), yielding complex $(X + Y)_{\kappa\lambda,n}^{\sigma'\tau'}$ with $\sigma'\tau' = \alpha\alpha, \beta\beta$ (parts with $\sigma'\tau' = \alpha\beta, \beta\alpha$ are not needed here)

$$(X + Y)_{\kappa\lambda,n}^{\sigma'\tau'} = \frac{1}{2} \sum_{j\bar{\sigma}'b\bar{\tau}'} (X + Y)_{j\bar{\sigma}'b\bar{\tau}',n} (c_{\kappa j\bar{\sigma}'}^{\sigma'} c_{\lambda b\bar{\tau}'}^{\tau'*} + c_{\kappa b\bar{\tau}'}^{\tau'} c_{\lambda j\bar{\sigma}'}^{\sigma'*}) \quad (27)$$

Third, the real symmetric (two-electron) Coulomb integrals $\langle \xi_\mu \xi_\kappa | \xi_\nu \xi_\lambda \rangle$ (in Dirac notation) are contracted with the complex $(X + Y)_{\kappa\lambda,n}^{\alpha\alpha} + (X + Y)_{\kappa\lambda,n}^{\beta\beta}$

$$(U + V)_{\mu\nu,n}^{\sigma\tau} = \sum_{\kappa\sigma'\lambda\tau'} \langle \xi_\mu \xi_\kappa | \xi_\nu \xi_\lambda \rangle \delta_{\sigma\tau} \delta_{\sigma'\tau'} (X + Y)_{\kappa\lambda,n}^{\sigma'\tau'} \quad (28)$$

In our code, the resolution of the identity (RI) approximation^{67,68} is utilized for the calculation of the (two-electron) Coulomb integrals. Last, the result of eq 28 is back-transformed to the spinor basis using a symmetric transformation (as in eq 27) by exploiting the symmetry of the (two-electron) Coulomb integrals. Thus, the left side of eq 22 is obtained ($\sigma\tau = \alpha\alpha, \beta\beta$) as

$$(\Phi_{i\bar{\sigma}}\Phi_{p\bar{0}}|\rho_{0n}) = \frac{1}{2} \sum_{\mu\sigma\nu\tau} (U + V)_{\mu\nu,n}^{\sigma\tau} (c_{\mu i\bar{\sigma}}^{\sigma*} c_{\nu p\bar{0}}^{\tau} + c_{\mu p\bar{0}}^{\tau} c_{\nu i\bar{\sigma}}^{\sigma*}) \quad (29)$$

It was ensured that the one-electron energies within the 2c G_0W_0 approximation are invariant under rotations in spin space and that the correct 1c limit is always obtained.

2c computations are more demanding with regard to computation time and required memory than 1c ones. In both the 1c and 2c G_0W_0 approximation, the computationally most demanding step is the calculation of *all* excitations within the RPA (TDH) method (Section 2.2), i.e., the *full* $O((N \cdot N^{\text{virt}})^3)$ -scaling diagonalization of Ω^{RPA} ; see eq 15. In the case of the 2c (Kramers-restricted) closed-shell treatment, an additional prefactor of 256 arises compared to the 1c closed-shell formalism, since the number of occupied and virtual molecular orbitals/spinors is doubled (factor $(2 \cdot 2)^3 = 64$), and a complex (Hermitian) diagonalization algorithm is needed instead of a real (symmetric) one (factor 4).

4. APPLICATIONS

4.1. Computational Details. All ground-state closed-shell structures of diatomic molecules and ZnF_2 were optimized using 1c DFT and the GGA functional of Becke and Perdew (BP86)^{69,70} in combination with polarized quadruple- ζ valence basis sets (dhf-QZVP-2c).⁷¹ The dhf-bases are optimized for usage in connection with Dirac–Hartree–Fock ECPs (dhf-ECPs), which account for scalar relativistic effects in 1c calculations and additionally for SOC effects in 2c calculations. For I and Ag, pseudopotentials (dhf-ECP-28)^{45,72} covering the inner 28 electrons, for Cs, a pseudopotential (dhf-ECP-46)⁴⁸ covering the inner 46 electrons, and for Bi, a pseudopotential (dhf-ECP-60)⁴⁶ covering the inner 60 electrons were used. Coordinates of all optimized structures are available as Supporting Information, Tables IV–VIII.

One-electron energies were computed at both the 2c and 1c levels using the GGA functional PBE,⁷³ Becke's three-parameter hybrid functional with Lee–Yang–Parr correlation (B3LYP),⁷⁴ the nonempirical hybrid functional PBE0,⁷⁵ HF theory, and the G_0W_0 approximation (linearized and self-consistent manner) based on PBE, B3LYP, PBE0, and HF orbitals/spinors and their energies. In G_0W_0 calculations, pure RPA screening was used, i.e., *all* excitations within the TDDFT formalism^{52,66} were considered using only the Coulomb contribution to the coupling matrix (eq 14), and η (eqs 8 and 18) was chosen to be 0.027 eV (0.001 hartree). Vertical first IEs (EAs) were additionally obtained by the difference of the self-consistently calculated total energies between cation (anion) and neutral system. As an approximation to G_0W_0 , the correlation contribution to the one-electron energies (obtained via RPA screening) was neglected ($\Sigma_c = 0$ in eq 19). The one-electron energies obtained within this approximation are

Table 1. Scalar Relativistic (1c) and Two-Component (2c) First Ionization Energies (IEs) of Seven Systems^a

method		Xe	Ba	Hg	I ₂	Bi ₂	AgI	CsI	MAE	SD
exp.		12.1 ⁹⁶	5.2 ⁹⁷	10.4 ⁹⁸	9.3 ⁹⁹	7.3 ¹⁰⁰	8.4 ¹⁰¹	7.2 ¹⁰²		
G ₀ W ₀ (HF)	1c	12.6	5.1	9.9	9.9	8.2	8.9	7.7	0.5	0.6
	2c	12.1	5.1	9.9	9.5	7.4	8.6	7.4	0.2	0.3
G ₀ W ₀ (PBE0)	1c	12.2	5.1	10.1	9.5	7.9	8.8	7.3	0.3	0.4
	2c	11.8	5.1	10.1	9.1	7.3	8.5	7.0	0.2	0.2
G ₀ W ₀ (B3LYP)	1c	12.2	5.0	10.1	9.4	8.0	8.8	7.2	0.2	0.4
	2c	11.8	5.0	10.1	9.1	7.3	8.5	7.0	0.2	0.2
G ₀ W ₀ (PBE)	1c	12.0	5.0	10.1	9.3	7.9	8.7	7.1	0.2	0.3
	2c	11.6	5.0	10.1	8.9	7.2	8.4	6.8	0.3	0.3
Δ -SCF(B3LYP)	1c	12.3	5.2	10.3	9.4	8.2	9.0	7.6	0.3	0.5
	2c	11.9	5.2	10.3	9.0	7.3	8.7	7.3	0.2	0.2
Δ -SCF(PBE)	1c	12.3	5.2	10.4	9.2	8.1	9.0	7.7	0.3	0.5
	2c	11.9	5.2	10.4	8.9	7.3	8.7	7.3	0.2	0.2
HF	1c	12.4	4.4	8.9	9.8	7.5	8.9	7.7	0.6	0.8
	2c	12.0	4.4	8.9	9.4	6.7	8.6	7.3	0.5	0.7
PBE0	1c	9.5	3.7	7.5	7.4	6.1	6.8	5.4	1.9	2.2
	2c	9.1	3.7	7.5	7.0	5.4	6.5	5.1	2.2	2.5
B3LYP	1c	9.1	3.5	7.4	7.1	5.9	6.6	5.1	2.2	2.4
	2c	8.7	3.5	7.4	6.7	5.2	6.3	4.8	2.5	2.7
PBE	1c	8.2	3.2	6.8	6.3	5.4	5.9	4.4	2.8	3.1
	2c	7.8	3.2	6.8	5.9	4.7	5.6	4.2	3.1	3.4
approx.(PBE)	1c	12.2	4.3	9.1	9.6	7.2	9.4	7.7	0.6	0.8
	2c	11.8	4.3	9.1	9.2	6.5	9.1	7.4	0.6	0.8
extrap.(B3LYP)	2c	11.8	5.0	10.1	9.1	7.3	8.5	7.0	0.2	0.2

^aAll calculated values were obtained using HF, the PBE0, B3LYP and PBE functional in combination with dhf-QZVP-2c basis sets and dhf-ecp-2c spin-orbit effective core potentials (ECPs). G₀W₀ calculations were done using pure RPA screening, i.e. only the Coulomb contribution to the coupling matrix in eq 14. Δ -SCF first IEs were obtained by the difference of the self-consistently calculated total energies between cation and neutral system. In case of “approximate G₀W₀(PBE)”, the correlation contribution to the one-electron energies was neglected. Furthermore, as an extrapolation (“extrapolated 2c G₀W₀(B3LYP)”), the 1c G₀W₀(B3LYP) first IE was corrected by the effect of spin-orbit coupling (SOC) via the difference between the 2c and 1c B3LYP results. MAE denotes the mean absolute error and SD the standard deviation. The IEs with maximum absolute errors for each method are marked bold. All values are in eV.

equivalent to the expectation value of the Fock operator using the KS reference orbitals/spinors. dhf-QZVP-2c basis sets were applied in all calculations, which are sufficiently large for most applications at the (correlated) G₀W₀ level.³² For Xe, a pseudopotential (dhf-ECP-28)⁴⁷ covering the inner 28 electrons, for Ba, a pseudopotential (dhf-ECP-46)⁴⁹ covering the inner 46 electrons, and for Hg, a pseudopotential (dhf-ECP-60)⁴⁵ covering the inner 60 electrons were used. For consideration of the core levels of Zn and ZnF₂, relativistic effects were included using the all-electron X2C approach⁴² in combination with the dhf-QZVP-2c basis set for F and a relativistic quadruple- ζ quality basis set for Zn, which was obtained by reoptimizing exponents and contraction coefficients of the nonrelativistic polarized quadruple- ζ valence basis set (def2-QZVP)⁷⁶ with (numerical) gradients of the energy at 1c X2C HF level and adding a set of 5 *p* functions,

which were roughly optimized by minimizing the energy at 2c X2C HF level; see Table 3 of the Supporting Information.

In all calculations, the RI approximation^{67,68} was employed for the Coulomb integrals. The applied auxiliary basis sets⁷⁷ are suited for bases optimized for dhf-ECPs.⁷⁸ In the case of X2C calculations on Zn, this auxiliary basis set was decontracted. The error of the RI approximation was tested for a set of 27 molecules at the 1c G₀W₀ level and found to be smaller than 0.1 eV.³² Reference-state energies and density matrices were converged to 10⁻¹⁰ au. At the DFT level, fine quadrature grids of size 5⁷⁹ were employed.

4.2. First Ionization Energies and Electron Affinities.

The 2c G₀W₀ method, based on different references (HF, PBE0, B3LYP, PBE), was applied for the calculation of first IEs (Table 1) and first EAs (Table 2) of several atomic and diatomic systems. In this subsection, we present only the results for the linearized G₀W₀ version to be consistent with ref 32;

Table 2. Scalar Relativistic (1c) and Two-Component (2c) First Electron Affinities (EAs) of Three Diatomic Molecules^a

method		I ₂	Bi ₂	CsI
exp.		2.5 ¹⁰³	1.2 ¹⁰⁴	0.6 ¹⁰⁵
G ₀ W ₀ (HF)	1c	1.7	1.1	0.5
	2c	1.7	1.2	0.5
G ₀ W ₀ (PBE0)	1c	1.8	1.1	0.3
	2c	1.8	1.2	0.3
G ₀ W ₀ (B3LYP)	1c	1.9	1.2	0.3
	2c	1.9	1.3	0.3
G ₀ W ₀ (PBE)	1c	2.0	1.2	0.3
	2c	1.9	1.4	0.3
Δ-SCF(B3LYP)	1c	1.7	1.0	0.5
	2c	1.7	1.1	0.5
Δ-SCF(PBE)	1c	1.7	1.0	0.6
	2c	1.7	1.1	0.6
HF	1c	0.6	0.4	0.3
	2c	0.6	0.3	0.3
PBE0	1c	3.7	2.8	1.3
	2c	3.7	2.9	1.3
B3LYP	1c	3.8	2.9	1.5
	2c	3.8	3.0	1.5
PBE	1c	4.5	3.3	1.8
	2c	4.4	3.5	1.8
approx.(PBE)	1c	0.3	0.1	−0.5
	2c	0.3	0.0	−0.5
extrap.(B3LYP)	2c	1.9	1.3	0.3

^aAll calculated values were obtained using HF, the PBE0, B3LYP and PBE functional in combination with dhf-QZVP-2c basis sets and dhf-ecp-2c spin-orbit effective core potentials (ECPs). Δ-SCF first EAs were obtained by the difference of the self-consistently calculated total energies between anion and neutral system. See Table 1 for further information. All values are in eV.

within the given accuracy, they are identical to the self-consistent G₀W₀ values. Results were compared to the 1c case, to the orbital/spinor energies of the reference state, to numbers obtained by forming the difference of PBE/B3LYP energies calculated for the ions and the neutral system, Δ-SCF(PBE)/Δ-SCF(B3LYP), and to the experiment. Furthermore, two comparably economic approximations were tested: (a) neglecting the electron correlation in the G₀W₀ treatment, in other words, the first-order correction of DFT (PBE) orbital/spinor energies toward HF orbital/spinor energies requiring only the setup of the Fock-matrix for a converged DFT calculation, “approximate G₀W₀(PBE)”, and (b) extrapolating the full 2c G₀W₀(B3LYP) result from 1c G₀W₀(B3LYP), 1c B3LYP, and 2c B3LYP, “extrapolated 2c G₀W₀(B3LYP)”; see below.

Results in Tables 1 and 2 may be summarized as follows. G₀W₀ and Δ-SCF are of similar accuracy; typical absolute errors for the 2c variants are in the range of 0 to 0.5 eV. This is significantly better than orbital energies from HF (typically more than 0.5 eV) or DFT (typically more than 2 eV). The differences between 1c and 2c approaches (see below) are smaller than these errors for most cases. Best among the G₀W₀ procedures is 2c G₀W₀(B3LYP), for IEs yielding a standard deviation (SD) of 0.2 eV and a maximum absolute error of 0.3 eV, which is a certain improvement over 1c G₀W₀(B3LYP) with respective values of 0.4 and 0.7 eV. It has to be noted that for the much cheaper Δ-SCF(PBE) and Δ-SCF(B3LYP) almost the same numbers (both at 1c and 2c levels) are obtained. Furthermore, the Δ-SCF values are almost identical for the two functionals. The same holds true for EAs. The even more economic procedure, approximate G₀W₀(PBE), yields results very similar to those with HF (as expected) for IEs, but the results are significantly worse than those with HF for EAs. The latter are close to zero for the three compounds under investigation. Obviously, starting from by far too high (up to about 2 eV) orbital/spinor energies of PBE, the first-order approach toward the HF orbital/spinor energies overestimates the required correction. Furthermore, the comparably small differences between the 1c and 2c approaches are almost invisible with this method. The extrapolated 2c G₀W₀(B3LYP) method (1c G₀W₀(B3LYP) minus 1c B3LYP plus 2c B3LYP), in contrast, almost exactly reproduces the numbers of the full 2c G₀W₀(B3LYP) treatment, as the difference between 1c and 2c treatments is almost the same for B3LYP and G₀W₀(B3LYP). Thus, SOC effects on one-electron energies for G₀W₀ are obtained by the costs of one additional 2c ground-state calculation. Also, for the other methods, the difference between 1c and 2c treatments is almost the same; they differ typically by less than 0.1 eV. It has to be noted that the influence of SOC effects on IEs is not very large; the maximum is observed for Bi₂, 0.7 eV; for Ba and Hg, where only *s*-orbitals are involved, it is zero. For clarity, we note that for the latter two cases all individual contributions to the G₀W₀ one-electron energies (see eq 19) are almost identical in the 1c and 2c treatments; see Table 1 of the Supporting Information. For EAs, SOC effects are even less important. The maximum is again observed for Bi₂, about 0.1 eV. We note that when using the experimental distance of 266.6 pm^{80,81}, instead of the 1c BP86/QZVP optimized distance of 269.3 pm for I₂, the IE decreases by 0.03 eV for 2c PBE and by 0.02 eV for 2c G₀W₀(PBE), and the EA by 0.10 eV for 2c PBE and by 0.11 eV for 2c G₀W₀(PBE). Similarly, upon using TDDFT instead of pure RPA screening (i.e., additionally considering the XC contribution to the coupling matrix in eq 14), as also done by van Setten et al.,³² the IE decreases by 0.03 eV, whereas the EA increases by 0.14 eV for the 2c G₀W₀(PBE) treatment of I₂.

So far, the advantage of G₀W₀ over Δ-SCF, at least for first IEs and first EAs, is not evident, in particular, if computational costs are compared to those of Δ-SCF. The latter requires two ground-state calculations needing on a single Intel Xeon X5650 2.67 GHz processor, e.g., for Bi₂ (238 basis functions, PBE) together 16 s (starting from Hückel orbitals) at the 1c and 58 s (starting from 1c orbitals) at the 2c level. G₀W₀ (presently) basically requires the calculation of all excitations (3887 at the 1c level, 15 548 at the 2c level) plus the comparably small effort for the reference-state calculation and the evaluation of eq 19. This needs 4 min 14 s at the 1c level and even 10 h 35 min at the 2c level and thus a 13 (650) times higher effort at the 1c

Table 3. Two-Component (2c) Average Binding Energies and Splittings for the $2p_j$ ($j = 1/2, 3/2$) Levels of Zn and ZnF_2^a

method	Zn		ZnF_2	
	average	splitting	average	splitting
exp.	1029.6 ¹⁰⁶	23.1 ¹⁰⁶	1030.5 ¹⁰⁷	≈23 ¹⁰⁸
G_0W_0 (HF)	1045.1 (1047.7)	27.6	1046.6 (1048.4)	27.3
G_0W_0 (PBE0)	1032.0 (1032.2)	23.3	1035.3 (1035.1)	24.4
G_0W_0 (B3LYP)	1030.9 (1031.2)	23.1	1032.9 (1034.1)	20.2
G_0W_0 (PBE)	1025.5 (1026.9)	20.7	1026.2 (1029.8)	14.6
G_0W_0 (HF)sc	1043.2 (1043.2)	25.9	1045.3 (1045.5)	25.9
G_0W_0 (PBE0)sc	1032.8 (1032.3)	25.8	1033.6 (1032.9)	25.9
G_0W_0 (B3LYP)sc	1030.8 (1030.3)	25.7	1034.3 (1034.6)	25.8
G_0W_0 (PBE)sc	1027.7 (1028.7)	25.5	1031.5 (1031.5)	25.7
HF	1065.1 (1064.9)	26.2	1067.1 (1067.0)	26.2
PBE0	1019.2 (1019.1)	25.5	1021.4 (1021.3)	25.5
B3LYP	1016.5 (1016.4)	25.5	1018.9 (1018.8)	25.5
PBE	1003.8 (1003.6)	25.3	1006.0 (1005.9)	25.3

^aAll calculated values were obtained using HF, the PBE0, B3LYP and PBE functional in combination with the X2C approach employing an all-electron relativistic quadruple- ζ quality basis set for Zn and a dhf-QZVP-2c basis set for F. G_0W_0 values were obtained from the linearized version as well as self-consistently (sc). See Table 1 for further information. Values in parentheses are scalar relativistic (1c) results for the $2p$ level. All values are in eV.

(2c) level for G_0W_0 compared to that with Δ -SCF. CPU times for 2c G_0W_0 are higher than for 1c G_0W_0 by a factor of about 150; the time for the diagonalization of the (full) matrix Ω^{RPA} (see eq 15) increases from 1 min 48 s at the 1c level to 7 h 49 min, which is a factor of 260, which is close to the expected value of 256; see Section 3.

Overall, accounting for SOC in the calculation of first IEs and EAs via 2c G_0W_0 has rather benchmark character, the extrapolation from the 1c G_0W_0 and the 2c ground-state calculations is by far more economic and yields almost the same numbers. Compared to the still more economic Δ -SCF, this extrapolation procedure has one advantage: for closed-shell systems, one avoids the calculation of open-shell ions, which sometimes are not easy to converge at the 2c level.

4.3. Core-Level Splittings. Different from Δ -SCF, G_0W_0 is also applicable for the calculation of the energies for ionization processes from inner orbitals, identified with the negative of the G_0W_0 one-electron energies of these levels, or, without G_0W_0 correction, with the negative of the orbital/spinor energy. As an example, we consider the average value and the SOC splitting of the $2p$ levels of the Zn atom and the ZnF_2 molecule (both with X2C), see Table 3, as well as the $5d$ level of the Hg atom (with dhf-ECP-60), see Table 4, obtained with the methods listed above (except for Δ -SCF). Additionally, the self-consistent (sc) version of G_0W_0 is used. Results are compared to the experiment.

First of all, core levels show a stronger dependence on the functional than IEs and EAs. This is true for G_0W_0 as well as for the references themselves. The effect is largest for the SOC splittings calculated with linearized G_0W_0 . As an example, for the Zn atom, 27.6 eV are obtained for G_0W_0 (HF) and 20.7 eV for G_0W_0 (PBE). G_0W_0 (B3LYP) and G_0W_0 (PBE0) are in-between, as expected. For the self-consistent G_0W_0 approach, in contrast, very similar splittings are observed for all references: 25.9 eV for G_0W_0 (HF)sc and 25.5 eV for G_0W_0 (PBE)sc. We thus discuss only the G_0W_0 sc results and the orbital/spinor energies (without G_0W_0 correction), at first for Zn, then for ZnF_2 , and finally for Hg. The splittings from G_0W_0 sc are very close to the splittings of the orbital/spinor energies, 26.2 eV for HF and 25.3 eV for PBE, and also close to the experimental value of 23.1 eV. Electron binding energies calculated from the

Table 4. Two-Component (2c) Binding Energies for the $5d_j$ ($j = 3/2, 5/2$) Levels of Hg^a

method	average	splitting
exp.	15.6	1.8
G_0W_0 (HF)	15.2 (15.2)	1.8
G_0W_0 (PBE0)	14.5 (14.5)	1.8
G_0W_0 (B3LYP)	14.5 (14.5)	1.8
G_0W_0 (PBE)	14.3 (14.2)	1.8
G_0W_0 (HF)sc	15.2 (15.2)	1.8
G_0W_0 (PBE0)sc	14.5 (14.4)	1.8
G_0W_0 (B3LYP)sc	14.5 (14.4)	1.8
G_0W_0 (PBE)sc	14.1 (14.0)	1.8
HF	16.4 (16.4)	2.0
PBE0	11.7 (11.7)	1.8
B3LYP	11.3 (11.3)	1.8
PBE	9.9 (9.9)	1.7

^aAll calculated values were obtained using HF, the PBE0, B3LYP and PBE functional in combination with dhf-QZVP-2c basis set and dhf-ecp-2c spin-orbit effective core potential (ECPs). G_0W_0 values were obtained from the linearized version as well as self-consistently (sc). See Table 1 for further information. Values in parentheses are scalar relativistic (1c) results for the $5d$ level. All values are in eV. Experimental results are from ref 109.

average of the 2c spinor energies range from 1065.1 eV (HF) to 1003.8 eV (PBE). For G_0W_0 sc, the differences are much smaller: 1043.2 eV for G_0W_0 (HF)sc and 1027.7 eV for G_0W_0 (PBE)sc. Hybrid functionals are in-between for both cases. Averaged 2c results and 1c values agree within about 1 eV. Furthermore, the experimental value of 1029.6 eV is met very well by G_0W_0 sc for references PBE, B3LYP, and PBE0 and reasonably also for HF. For ZnF_2 , the experimentally observed SOC splitting is the same as that for the Zn atom; the average electron binding energy increases by about 1 eV. Both facts are reproduced by both the orbital/spinor energies and the G_0W_0 sc approach. The increase of the average electron binding energy is somewhat overestimated.

For the $5d$ level of Hg, the experimental splitting of 1.8 eV is obtained by all G_0W_0 sc procedures; also, for the orbital/spinor energies, very reasonable agreement is obtained (1.7–2.0 eV). The averaged 2c as well as the 1c binding energies obtained

from orbital/spinor energies range from 16.4 eV (HF) to 9.9 eV (PBE). For G_0W_0 sc, in contrast, almost the same values are obtained for all references, and the averaged 2c binding energies are virtually identical to the 1c binding energies. The deviation to the experiment is about 1 eV.

Thus, the reliability of the extrapolated 2c G_0W_0 technique (see above) is also confirmed here: the G_0W_0 sc averaged 2c binding energies and the G_0W_0 sc 1c binding energies are very similar and closer to the experimental data than the respective orbital energies. Furthermore, the values for the SOC splittings from spinor energies are not significantly changed by the G_0W_0 sc approach.

5. CONCLUSIONS

We presented the two-component extension of the G_0W_0 method for closed-shell systems based on the previously implemented one-component version in TURBOMOLE that uses localized basis functions. In this way it is, to the best of our knowledge for the first time, possible to account for spin–orbit effects on one-electron energies of isolated molecular systems at G_0W_0 level. We briefly sketched the derivation of the underlying equations and gave details about the implementation. The method was applied to several atomic and small molecular systems based on different references: HF, PBE, B3LYP, and PBE0 (with results very similar to those with B3LYP). The influence of spin–orbit coupling changes one-electron energies for the highest occupied level, which are identified with experimentally determined first ionization energies by up to 0.7 eV. Changes are almost the same for G_0W_0 with different references and for the orbital energies of the references themselves. Thus, we proposed an economic extrapolation scheme based on the one-component G_0W_0 (B3LYP) and the two-component B3LYP calculation that yields virtually identical ionization energies as those with the full two-component G_0W_0 (B3LYP) procedure and shows errors with respect to the experiment of 0.3 eV at most. The same is true for electron affinities, but the maximum difference to the experiment is larger, 0.6 eV. It has to be noted that G_0W_0 is much more expensive than Δ -SCF, which is of about the same accuracy for first ionization energies and electron affinities. For binding energies of core levels, in contrast, Δ -SCF is not applicable. The self-consistently obtained G_0W_0 averaged two-component binding energies and the respective one-component binding energies are very similar and closer to the experimental data than the corresponding orbital/spinor energies. Furthermore, the values for the splittings from spinor energies are not significantly changed by the self-consistent G_0W_0 approach. Thus, like for the first ionization energies, the best cost–benefit ratio is obtained with the extrapolation mentioned above.

■ APPENDIX

Connection to Total Ground-State Correlation Energies from the Two-Component Random Phase Approximation

In this work, the effect of electron correlation along with SOC on one-electron energies was included within the 2c GW method. It has been shown previously that, in the 1c case, the GW method is strongly related to RPA,^{82–87} which includes the effect of electron correlation on total ground-state energies at the same level of theory.^{88,89} In this Appendix, we show how total correlation energies under the influence of SOC from the 2c RPA⁵³ can be expressed in terms of the basic quantities also

used in Section 2 for the derivation of one-electron energies within the 2c GW (or 2c G_0W_0) approach: the transition densities (eq 17) and excitation energies (eq 15) or the density–density response function (eq 18).

The starting point for 2c RPA usually is the 2c adiabatic connection Hamiltonian^{53,90,91}

$$\hat{H}^\alpha = \hat{T}\mathbf{1} + \hat{V}^\alpha[\rho] + \alpha\hat{V}_{ee}\mathbf{1} \quad (30)$$

\hat{T} is the many-electron analog of \hat{t} in eq 1, and \hat{V}_{ee} is the many-electron analog of \hat{v}_{ee} in eq 4, which is scaled by a dimensionless coupling strength parameter α . $\hat{V}^\alpha[\rho]$ is the many-electron analog of \hat{v} in eq 1 containing the 2c SOC contribution, and constrains the ground state Ψ_0^α to yield the interacting ground state density ρ for all α .⁹² $\alpha = 0$ corresponds to the non-interacting KS system, which is described by the 2c KS Slater determinant $\Psi_0^{\alpha=0}$.

The total ground-state correlation energy E_C is exactly given by a coupling strength integral

$$E_C = \int_0^1 d\alpha \sum_n (E_H[\rho_{0n}^\alpha] - E_H[\rho_{0n}^0]) \quad (31)$$

with the real Hartree energy functional

$$E_H[\rho_{0n}^\alpha] = \frac{1}{2} \int d^3r_1 d^3r_2 \hat{v}_{ee}(\vec{r}_1 - \vec{r}_2) \rho_{0n}^\alpha(\vec{r}_1) (\rho_{0n}^\alpha(\vec{r}_2))^* \quad (32)$$

Thus, E_C can be expressed entirely in terms of one-electron transition densities. These one-electron transition densities ρ_{0n}^α are accessible from 2c RPA (2c TDH theory) (as $\rho_{0n}^{\alpha\text{RPA}}$) as described in Section 2.2 with the coupling matrix in eq 14 scaled by the coupling strength α .⁵³

Alternatively, using the (zero-temperature) fluctuation–dissipation theorem⁹³

$$\sum_n \rho_{0n}^{\alpha\text{RPA}}(\vec{r}_1) (\rho_{0n}^{\alpha\text{RPA}}(\vec{r}_2))^* = - \int_0^\infty \frac{d\nu}{\pi} \mathcal{I}[\chi^{\alpha\text{RPA}}(\vec{r}_1, \vec{r}_2, \nu)] \quad (33)$$

the total ground-state correlation energy E_C^{RPA} within 2c RPA can be rewritten in terms of a frequency integral with the density–density response function (eq 18) at coupling strength α .^{90,94}

$$E_C^{\text{RPA}} = -\frac{1}{2} \int_0^1 d\alpha \int_0^\infty \frac{d\nu}{\pi} \int d^3r_1 d^3r_2 \hat{v}_{ee}(\vec{r}_1 - \vec{r}_2) \times \mathcal{I}[\chi^{\alpha\text{RPA}}(\vec{r}_1, \vec{r}_2, \nu) - \chi^{\text{ORPA}}(\vec{r}_1, \vec{r}_2, \nu)] \quad (34)$$

\mathcal{I} denotes the imaginary part. The central quantity in eq 34, the density–density response function from eq 18, is also used to describe the effect of electron correlation on one-electron energies $\epsilon_{p\bar{v}}^{G_0W_0}$ within the 2c G_0W_0 method: the final expression for the $\epsilon_{p\bar{v}}^{G_0W_0}$, eq 19, contains the 2c self energy Σ from eq 7, which depends on the dynamically screened Coulomb interaction W . Finally, the latter is defined in eq 9 in terms of the density–density response function.

Finally, a simple result for E_C^{RPA} is obtained by carrying out the coupling strength integration analytically

$$E_C^{\text{RPA}} = \frac{1}{2} \sum_n (\omega_n^{\text{RPA}} - \omega_n^{\text{TDA RPA}}) \quad (35)$$

This so-called plasmon formula⁸² expresses E_C^{RPA} in terms of a sum over all excitation energies ω_n^{RPA} calculated according to eq

15 (at full coupling strength, $\alpha = 1$) and all excitation energies $\omega_n^{\text{TDA RPA}}$ obtained within the Tamm–Dancoff approximation (TDA),⁹⁵ neglecting Y^{RPA} in eq 10.⁵³

■ ASSOCIATED CONTENT

■ Supporting Information

All-electron relativistic quadruple- ζ quality basis set for Zn. Coordinates of all structures. This material is available free of charge via the Internet at <http://pubs.acs.org>.

■ AUTHOR INFORMATION

Corresponding Author

*E-mail: florian.weigend@kit.edu.

Funding

M.K. is funded by the Carl Zeiss Foundation and also thanks TURBOMOLE GmbH for financial support.

Notes

The authors declare no competing financial interest.

■ ACKNOWLEDGMENTS

The authors thank Michiel van Setten and Ferdinand Evers for useful discussion.

■ REFERENCES

- (1) Koopmans, T. *Physica* **1934**, *1*, 104–113.
- (2) Perdew, J. P.; Parr, R. G.; Levy, M.; Balduz, J. L. *J. Phys. Rev. Lett.* **1982**, *49*, 1691–1694.
- (3) Perdew, J. P.; Levy, M. *Phys. Rev. Lett.* **1983**, *51*, 1884–1887.
- (4) Perdew, J. P.; Levy, M. *Phys. Rev. B* **1997**, *56*, 16021–16028.
- (5) Hedin, L. *J. Phys.: Condens. Matter* **1999**, *11*, R489–R528.
- (6) Chong, D.; Gritsenko, O.; Baerends, E. J. *J. Chem. Phys.* **2002**, *116*, 1760–1772.
- (7) Gritsenko, O.; Baerends, E. J. *Can. J. Chem.* **2009**, *87*, 1383–1391.
- (8) Hedin, L. *Phys. Rev.* **1965**, *139*, A796–A823.
- (9) Onida, G.; Reining, L.; Rubio, A. *Rev. Mod. Phys.* **2002**, *74*, 601–659.
- (10) Bechstedt, F.; Fuchs, F.; Kresse, G. *Phys. Status Solidi B* **2009**, *246*, 1877–1892.
- (11) Rocca, D.; Vörös, M.; Gali, A.; Galli, G. *J. Chem. Theory Comput.* **2014**, *10*, 3290–3298.
- (12) Grossman, J. C.; Rohlfing, M.; Mitas, L.; Louie, S. G.; Cohen, M. L. *Phys. Rev. Lett.* **2001**, *86*, 472–475.
- (13) Ethridge, E. C.; Fry, J. L.; Zaidar, M. *Phys. Rev. B* **1996**, *53*, 3662–3668.
- (14) Tiago, M.; Chelikowsky, J. R. *Phys. Rev. B* **2006**, *73*, 205334.
- (15) Rostgaard, C.; Jacobsen, K. W.; Thygesen, K. S. *Phys. Rev. B* **2010**, *81*, 085103.
- (16) Ke, S. *Phys. Rev. B* **2011**, *84*, 205415.
- (17) Blase, X.; Attaccalite, C.; Olevano, V. *Phys. Rev. B* **2011**, *83*, 115103.
- (18) Baumeier, B.; Andrienko, D.; Ma, Y.; Rohlfing, M. *J. Chem. Theory Comput.* **2012**, *8*, 997–1002.
- (19) Sharifzadeh, S.; Tamblyn, I.; Doak, P.; Darancet, P. T.; Neaton, J. B. *Eur. Phys. J. B* **2012**, *85*, 323.
- (20) Lopez del Puerto, M.; Tiago, M.; Chelikowsky, J. R. *Phys. Rev. Lett.* **2006**, *97*, 096401.
- (21) Lopez del Puerto, M.; Tiago, M.; Chelikowsky, J. R. *Phys. Rev. B* **2008**, *77*, 045404.
- (22) Ramos, L.; Paier, J.; Kresse, G.; Bechstedt, F. *Phys. Rev. B* **2008**, *78*, 195423.
- (23) Pavlyukh, Y.; Hübner, W. *Phys. Lett. A* **2004**, *327*, 241–246.
- (24) Noguchi, Y.; Ishii, S.; Ohno, K.; Sasaki, T. *J. Chem. Phys.* **2008**, *129*, 104104.
- (25) Bruneval, F. *Phys. Rev. Lett.* **2009**, *103*, 176403.
- (26) Tiago, M. L.; Idrobo, J. C.; Ögüt, S.; Jellinek, J.; Chelikowsky, J. R. *Phys. Rev. B* **2009**, *79*, 155419.
- (27) Adachi, H.; Ishii, S.; Ohno, K.; Ichinoseki, K.; Kawazoe, Y. *Mater. Trans.* **2006**, *47*, 2620–2623.
- (28) Ren, X.; Rinke, P.; Blum, V.; Wieferink, J.; Tkatchenko, A.; Sanfilippo, A.; Reuter, K.; Scheffler, M. *New J. Phys.* **2012**, *14*, 053020.
- (29) Foerster, D.; Koval, P.; Sanchez-Portal, D. *J. Chem. Phys.* **2011**, *135*, 074105.
- (30) Bruneval, F. *J. Chem. Phys.* **2012**, *136*, 194107.
- (31) Blum, V.; Gehrke, R.; Hanke, F.; Havu, P.; Havu, V.; Ren, X.; Reuter, K.; Scheffler, M. *Comput. Phys. Commun.* **2009**, *180*, 2175–2196.
- (32) van Setten, M. J.; Weigend, F.; Evers, F. *J. Chem. Theory Comput.* **2013**, *9*, 232–246.
- (33) Local version of TURBOMOLE V6.6 2014, a development of University of Karlsruhe and Forschungszentrum Karlsruhe GmbH, 1989–2007, TURBOMOLE GmbH since 2007.
- (34) Kutzelnigg, W.; Liu, W. *J. Chem. Phys.* **2005**, *123*, 241102.
- (35) Kutzelnigg, W.; Liu, W. *Mol. Phys.* **2006**, *104*, 2225–2240.
- (36) Liu, W.; Kutzelnigg, W. *J. Chem. Phys.* **2007**, *126*, 114107.
- (37) Liu, W.; Peng, D. *J. Chem. Phys.* **2006**, *125*, 044102.
- (38) Peng, D.; Liu, D.; Xiao, Y.; Cheng, L. *J. Chem. Phys.* **2007**, *127*, 104106.
- (39) Iliaš, M.; Saue, T. *J. Chem. Phys.* **2007**, *126*, 064102.
- (40) Peng, D.; Reiher, M. *Theor. Chem. Acc.* **2012**, *131*, 1081.
- (41) Peng, D.; Reiher, M. *J. Chem. Phys.* **2012**, *136*, 244108.
- (42) Peng, D.; Middelndorf, N.; Weigend, F.; Reiher, M. *J. Chem. Phys.* **2013**, *138*, 184105.
- (43) Peterson, K. A.; Figgen, D.; Dolg, M.; Stoll, H. *J. Chem. Phys.* **2007**, *126*, 124101.
- (44) Figgen, D.; Peterson, K. A.; Dolg, M.; Stoll, H. *J. Chem. Phys.* **2009**, *130*, 164108.
- (45) Figgen, D.; Rauhut, G.; Dolg, M.; Stoll, H. *Chem. Phys.* **2005**, *311*, 227–244.
- (46) Metz, B.; Stoll, H.; Dolg, M. *J. Chem. Phys.* **2000**, *113*, 2563–2569.
- (47) Peterson, K. A.; Figgen, D.; Goll, E.; Stoll, H.; Dolg, M. *J. Chem. Phys.* **2003**, *119*, 11113–11123.
- (48) Lim, I. S.; Schwerdtfeger, P.; Metz, B.; Stoll, H. *J. Chem. Phys.* **2005**, *122*, 104103.
- (49) Lim, I. S.; Stoll, H.; Schwerdtfeger, P. *J. Chem. Phys.* **2006**, *124*, 034107.
- (50) Armbruster, M. K.; Weigend, F.; van Wüllen, C.; Klopper, W. *Phys. Chem. Chem. Phys.* **2008**, *10*, 1748–1756.
- (51) Bischoff, F.; Klopper, W. *J. Chem. Phys.* **2010**, *132*, 094108.
- (52) Kühn, M.; Weigend, F. *J. Chem. Theory Comput.* **2013**, *9*, 5341–5348.
- (53) Kühn, M. *J. Chem. Theory Comput.* **2014**, *10*, 623–633.
- (54) Aryasetiawan, F.; Biermann, S. *Phys. Rev. Lett.* **2008**, *100*, 116402.
- (55) Aryasetiawan, F.; Biermann, S. *J. Phys.: Condens. Matter* **2009**, *21*, 064232.
- (56) Sakuma, R.; Friedrich, C.; Miyake, T.; Bügel, S.; Aryasetiawan, F. *Phys. Rev. B* **2011**, *84*, 085144.
- (57) Kutepov, A.; Haule, K.; Savrasov, S. Y.; Kotliar, G. *Phys. Rev. B* **2012**, *85*, 155129.
- (58) Umari, P.; Mosconi, E.; De Angelis, F. *Sci. Rep.* **2014**, *4*, 4467.
- (59) van Wüllen, C. *J. Comput. Chem.* **2002**, *23*, 779–785.
- (60) Hybertsen, M. S.; Louie, S. G. *Phys. Rev. Lett.* **1985**, *55*, 1418–1421.
- (61) Godby, R. W.; Schlüter, M.; Sham, L. J. *Phys. Rev. Lett.* **1986**, *56*, 2415–2418.
- (62) Furche, F. *J. Chem. Phys.* **2001**, *114*, 5982–5992.
- (63) Wang, F.; Ziegler, T.; van Lenthe, E.; van Gisbergen, S.; Baerends, E. J. *J. Chem. Phys.* **2005**, *122*, 204103.
- (64) Peng, D.; Zou, W.; Liu, W. *J. Chem. Phys.* **2005**, *123*, 144101.
- (65) Fetter, A. L.; Walecka, J. D. *Quantum Theory of Many-Particle Systems*; McGraw-Hill: New York, 1971.

- (66) Bauernschmitt, R.; Ahlrichs, R. *Chem. Phys. Lett.* **1996**, 256, 454–464.
- (67) Bauernschmitt, R.; Häser, M.; Treutler, O.; Ahlrichs, R. *Chem. Phys. Lett.* **1997**, 264, 573–578.
- (68) Eichkorn, K.; Weigend, F.; Treutler, O.; Ahlrichs, R. *Theor. Chem. Acc.* **1997**, 97, 119–124.
- (69) Becke, A. D. *Phys. Rev. A* **1988**, 38, 3098–3100.
- (70) Perdew, J. P. *Phys. Rev. B* **1986**, 33, 8822–8824.
- (71) Weigend, F.; Baldes, A. *J. Chem. Phys.* **2010**, 133, 174102.
- (72) Peterson, K. A.; Shepler, B. C.; Figgen, D.; Stoll, H. *J. Phys. Chem. A* **2006**, 110, 13877.
- (73) Perdew, J. P.; Burke, K.; Ernzerhof, M. *Phys. Rev. Lett.* **1996**, 77, 3865–3868.
- (74) Becke, A. D. *J. Chem. Phys.* **1993**, 98, 5648–5652.
- (75) Perdew, J. P.; Ernzerhof, M.; Burke, K. *J. Chem. Phys.* **1996**, 105, 9982–9985.
- (76) Weigend, F.; Ahlrichs, R. *Phys. Chem. Chem. Phys.* **2005**, 7, 3297.
- (77) Weigend, F. *Phys. Chem. Chem. Phys.* **2006**, 8, 1057–1065.
- (78) Armbruster, M. K.; Klopper, W.; Weigend, F. *Phys. Chem. Chem. Phys.* **2006**, 8, 4862–4865.
- (79) Treutler, O.; Ahlrichs, R. *J. Chem. Phys.* **1995**, 102, 346–354.
- (80) Huber, K. P.; Herzberg, G. *Molecular Spectra and Molecular Structure*; Van Nostrand and Reinhold: New York, 1979; Vol. IV.
- (81) Howard, W. F., Jr.; Andrews, L. *J. Raman Spectrosc.* **1974**, 2, 447–462.
- (82) Eshuis, H.; Bates, J. E.; Furche, F. *Theor. Chem. Acc.* **2012**, 131, 1084.
- (83) Jansen, G.; Liu, R.-F.; Ángyán, J. G. *J. Chem. Phys.* **2010**, 133, 154106.
- (84) Ángyán, J. G.; Liu, R.-F.; Toulouse, J.; Jansen, G. *J. Chem. Theory Comput.* **2011**, 7, 3116–3130.
- (85) Heßelmann, A.; Görling, A. *Mol. Phys.* **2011**, 109, 2473–2500.
- (86) Ren, X.; Pinke, P.; Joas, C.; Scheffler, M. *J. Mater. Sci.* **2012**, 47, 7447–7471.
- (87) Rekkedal, J.; Coriani, S.; Iozzi, M. F.; Teale, A. M.; Helgaker, T.; Pedersen, T. B. *J. Chem. Phys.* **2013**, 139, 081101.
- (88) Hellgren, M.; von Barth, U. *Phys. Rev. B* **2007**, 76, 075107.
- (89) Toulouse, J.; Zhu, W.; Ángyán, J. G.; Savin, A. *Phys. Rev. A* **2010**, 82, 032502.
- (90) Langreth, D. C.; Perdew, J. P. *Solid State Commun.* **1975**, 17, 1425–1429.
- (91) Gunnarsson, O.; Lundqvist, B. I. *Phys. Rev. B* **1976**, 13, 4274–4298.
- (92) Levy, M. *Proc. Natl. Acad. Sci. U.S.A.* **1979**, 76, 6062–6065.
- (93) Callen, H. B.; Welton, T. A. *Phys. Rev.* **1951**, 83, 34–40.
- (94) Langreth, D. C.; Perdew, J. P. *Phys. Rev. B* **1977**, 15, 2884–2901.
- (95) Hirata, S.; Head-Gordon, M. *Chem. Phys. Lett.* **1999**, 314, 291–299.
- (96) Schafer, H.; Rabenack, H. Z. *Anorg. Allg. Chem.* **1987**, 545, 224–226.
- (97) Rauh, E. G.; Ackermann, R. J. *J. Chem. Phys.* **1979**, 70, 1004–1007.
- (98) Hoareau, A.; Cabaud, B.; Mélinon, P. *Surf. Sci.* **1981**, 106, 195–203.
- (99) Cockett, M. C. R.; Donovan, R. J.; Lawley, K. P. *J. Chem. Phys.* **1996**, 105, 3347–3360.
- (100) Yoo, R. K.; Ruscic, B.; Berkowitz, J. *J. Chem. Phys.* **1993**, 99, 8445–8450.
- (101) Berkowitz, J. *Adv. High Temp. Chem.* **1971**, 3, 123–176.
- (102) Viswanathan, R.; Hilpert, K. *Ber. Bunsen-Ges.* **1984**, 88, 125–131.
- (103) Zanni, M. T.; Taylor, T. R.; Greenblatt, J.; Soep, B.; Neumark, D. M. *J. Chem. Phys.* **1997**, 107, 7613–7619.
- (104) Sun, Z.; Sun, S. T.; Liu, H. T.; Zhu, Q. H.; Gao, Z.; Tang, Z. C. *J. Phys. Chem. A* **2009**, 113, 8045–8054.
- (105) Miller, T. M.; Leopold, D. G.; Murray, K. K.; Lineberger, W. C. *J. Chem. Phys.* **1986**, 85, 2368–2375.
- (106) Schön, G. *J. Electron Spectrosc. Relat. Phenom.* **1973**, 2, 75–86.
- (107) Wagner, C. D. *Discuss. Faraday Soc.* **1975**, 60, 291–300.
- (108) Rosencwaig, A.; Wertheim, G. K.; Guggenheim, H. J. *Phys. Rev. Lett.* **1971**, 27, 479–481.
- (109) Svensson, S.; Martensson, N.; Basilier, E.; Malmqvist, P. A.; Gelius, U.; Siegbahn, K. *J. Electron Spectrosc. Relat. Phenom.* **1976**, 9, 51–65.